PHYSICAL REVIEW B **75**, 241308(R) (2007)

Vanishing of inhomogeneous spin relaxation in InAs-based field-effect transistor structures

Munekazu Ohno[1] and Kanji Yoh[1,2]
[1]*Research Center for Integrated Quantum Electronics, Hokkaido University, Sapporo 060-8628, Japan*
[2]*CREST-JST, Kawaguchi, Saitama 332-0022, Japan*
(Received 14 May 2007; published 26 June 2007)

The D'yakonov-Perel' spin relaxation process in the (001) InAs quantum well system is studied based on Monte Carlo (MC) simulation. The present space-resolved MC analysis demonstrates that the relaxation of spins oriented in any axes is totally suppressed with equal strength of Rashba and Dresselhaus effects, which is in marked contrast with the spin relaxation anisotropy reported previously in time-resolved analyses. Our calculation also shows a substantial contribution of the cubic term of the wave number vector in the Dresselhaus model onto the spatial spin distribution.

DOI: 10.1103/PhysRevB.75.241308 PACS number(s): 72.25.Rb, 72.25.Dc, 85.75.Hh

Carrier spin transport in a zinc-blende semiconductor involves decay of spin polarization coherence, i.e., a spin relaxation process due to several mechanisms[1–4] and suppression of the spin relaxation process is a prerequisite for realizing spintronics devices such as the spin-field-effect transistor (spin-FET).[5,6] At room temperature, among several mechanisms, electron spin relaxation due to the D'yakonov-Perel' (DP) mechanism is the most dominant in a quantum well (QW) system grown on (001) substrate. In an asymmetric QW system, bulk-inversion asymmetry (BIA) and structure-inversion asymmetry (SIA) lead to the Dresselhaus[7] and Rashba[8] spin-orbit terms in the effective Hamiltonian, respectively, and their corresponding effective magnetic fields are involved in the DP process. It has been demonstrated in several theoretical works[9–13] that the interplay between the Dresselhaus and Rashba effects causes a spin relaxation anisotropy so that the spin relaxation rate largely depends on the orientation of spin. The existence of such an anisotropy has been in fact confirmed by means of Hanle effect measurements in a recent work.[14] Of particular importance in these theoretical findings is that when the Rashba and Dresselhaus linear-in-**k** terms have equal strength, the relaxation of spin oriented in one of the $\langle 110 \rangle$ axes, more specifically the [110] axis within the present discussion, is totally suppressed, while the relaxation time of spins along the other axis is finite. Hence, it has been generally acknowledged that the spin along a different axis from [110] is not robust against the spin relaxation. The strong suppression of spin relaxation along [110] is the essential ingredient for nonballistic spin-FET proposed in Ref. 5.

The spin relaxation essentially proceeds in both temporal and spatial coordinates. In the theoretical works mentioned above, the spin relaxation anisotropy has been discussed only in a time-resolved analysis with the assumption of a homogeneous spin distribution. Based on a semiclassical Monte Carlo (MC) approach of spin transport,[15–18] in the present study, it is demonstrated that the time-resolved analysis can highlight only one aspect of anisotropic spin relaxation phenomena, overlooking an important feature inherent in the spin transport, i.e., spatial coherence of spin polarization. The present space-resolved MC simulation reveals that the relaxation of spins oriented in any axes is totally suppressed with equal strength of the Rashba and Dresselhaus effects, supporting the existence of a persistent spin helix (PSH) pattern recently predicted in Ref. 19. Further attention will be directed to the effect of the cubic term of the Dresselhaus model on the PSH pattern as well as the homogeneous spin distribution.

For the (001) QW system with spatial coordinates of $x \| [100]$ and $y \| [010]$, the BIA effective magnetic field $\Omega_{BIA}(\mathbf{k})$ is described in leading order by the Dresselhaus model, $\Omega_{BIA}(\mathbf{k}) = (2\gamma/\hbar)(k_x(k_y^2 - \langle k_z^2 \rangle), k_y(\langle k_z^2 \rangle - k_x^2), 0)$,[7] where $\langle k_z^2 \rangle$ is the expectation value with respect to the subband wave function in the QW and γ is the Dresselhaus parameter which is material dependent. The Rashba term of SIA spin splitting is represented as $\Omega_{SIA}(\mathbf{k}) = (2\alpha/\hbar)(k_y, -k_x, 0)$,[8] where α corresponds to the Rashba parameter depending on the material and also on the asymmetry of the QW in the growth direction and thus controlled by an external electric field along growth direction [gate voltage in the spin-FET (Ref. 5)]. The quantum mechanical evolution of the spin polarization vector **S** can be described by an evolution equation of classical momentum under the effective magnetic field, $d\mathbf{S}/dt = \Omega_{eff}(\mathbf{k}) \times \mathbf{S}$.[15,16] During free flight motion of the electron, the spin precession occurs along the **k**-dependent effective magnetic field. The MC simulation of carrier transport describes the evolution of the wave vector during multiple-scattering events and, hence, this allows direct observation of the DP spin relaxation process. As is common in reported MC simulations,[15–18] the reciprocal effect of spin on the electron motion through spin-orbit coupling is neglected in the present calculations. In the following, the spin polarization vector is described in the [110], $[1\bar{1}0]$, and [001] coordinate system and the corresponding vector components are denoted by S_+, S_-, and S_z, respectively.

The MC simulation is applied to the DP process at 300 K in a (001) InAs QW of 80 Å well width inserted between an $In_{0.53}Ga_{0.47}As$ subchannel and $Al_{0.48}In_{0.52}As$ barrier layer, which is quite similar to one of the most promising structures for realizing spin-FETs.[20] We performed the ensemble MC simulation of 4×10^4 electrons in the two-dimensional electron gas (2DEG) system, taking into account elastic scattering events originating from polar optical phonon, acoustic phonon, and remote impurities.[21] The carrier mobility at the low-field regime is calculated to be 9.5×10^3 cm^2/(V s) which is comparable to 9.3×10^3 cm^2/(V s) experimentally measured for the similar structure.[20]

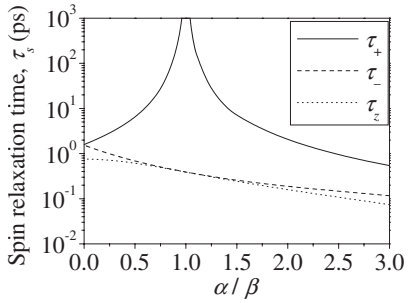

FIG. 1. Dependence of the spin relaxation time τ_s on the RD ratio α/β with different initial spin polarizations.

As described above, the strengths of Dresselhaus and Rashba effects are determined by the constants γ and α, respectively. The Dresselhaus parameter γ is set to 71×10^{-30} eV m^3 (Ref. 22) in all calculations of this study and then the constant β given as $\beta=\gamma\langle k_z^2\rangle$ is calculated to be 10.9×10^{-12} eV m for the present QW system. As for the Rashba parameter α, we systematically vary this value, using a ratio of α/β which is termed the Rashba Dresselhaus (RD) ratio here.

The spin polarization vector of each electron is a function of the space and time coordinates as explicitly denoted by $\mathbf{S}(\mathbf{r},t)$. As pointed out in Ref. 15, several types of spin relaxation measurements can be considered. One of the most commonly used ways is the time-resolved measurement in which the temporal evolution of spin polarization averaged over spatial coordinates, $\langle\mathbf{S}\rangle_R$, is the main concern.[15–17] The temporal evolution of such an averaged quantity is conventionally described to be an exponential decay with characteristic spin relaxation time. The present MC result for the dependence of the spin relaxation time on the RD ratio is shown in Fig. 1. The initial spin polarization of all the electrons at $t=0$ was assumed to be homogeneously oriented in one of three axes [110], $[1\bar{1}0]$, and [001] and, in this figure, τ_s with $s=+$, $-$, and z characterizes the spin relaxation process starting from the initial spin state oriented in [110], $[1\bar{1}0]$, and [001] axes, respectively. In order to simplify the discussion, the cubic term in the Dresselhaus model is omitted in this calculation. Several theoretical works have consistently predicted the relation $\tau_+=C/(\alpha-\beta)^2$, $\tau_-=C/(\alpha+\beta)^2$, and $\tau_z=C/[2(\alpha^2+\beta^2)]$ with a constant C (Refs. 9–12) and the present MC result is in full agreement with this relation. The divergent behavior of τ_+ at $\alpha/\beta=1.0$ can be explained by the fact that when the relation $\alpha/\beta=1.0$ is realized, the effective magnetic field is oriented in the [110] axis irrespective of $\mathbf{k}$, leading to no precession motion of the spin along [110]. The electron scattering events thus do not cause the spin relaxation for spin along [110].[5] On the other hand, the precession motion involved in spins oriented in the other axis results in the finite value of τ_- and τ_z in Fig. 1. Therefore, it has been recognized that the spin along a different axis from [110] is not robust against the spin relaxation, compared with the spin along [110].

Figure 2(a) shows the temporal evolution process of $\langle\mathbf{S}\rangle_R$ at $\alpha/\beta=1.0$ following homogenous distribution of spin along $[1\bar{1}0]$ at $t=0$. One can clearly see the decay of the spin

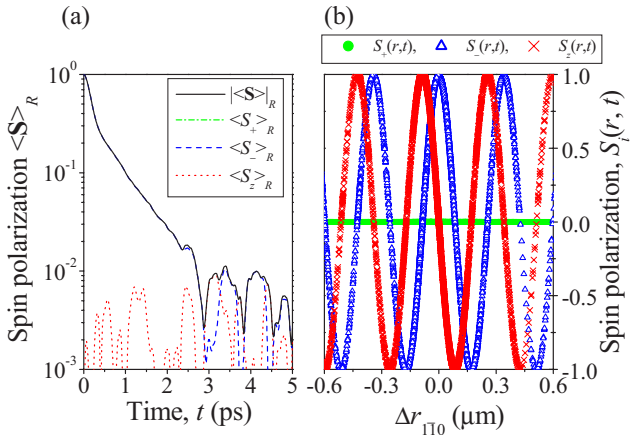

FIG. 2. (Color online) (a) Temporal evolution of the spatially averaged spin polarization vector at $\alpha/\beta=1.0$ with initial spin oriented in $[1\bar{1}0]$. (b) Projection of the spin polarization components $\mathbf{S}(r,t)$ of 100 electrons with respect to their net moving distances along the $[1\bar{1}0]$ direction, $\Delta r_{1\bar{1}0}=r_{1\bar{1}0}(t)-r_{1\bar{1}0}(0)$.

polarization.[23] Demonstrated in Fig. 2(b) is the projection of $\mathbf{S}(r,t)$ along the $[1\bar{1}0]$ spatial axis during the temporal evolution process in Fig. 2(a). The spin polarization components of 10^2 electrons, which were randomly chosen from 4×10^4 electrons, are plotted with respect to the net moving distance of each electron along the $[1\bar{1}0]$ spatial axis at several time instants. In this figure, it can be clearly seen that there exists a spatial oscillation of the spin polarization without any decoherence. From the evolution equation of spin precession motion, the rotation angle of spin during a certain time period Δt is given by $\theta=|\Omega(\mathbf{k})|\Delta t$. When the relation $\alpha=\beta$ is realized, the rotation angle is then expressed within linear-in-$\mathbf{k}$ terms as $\theta=(4\alpha m^*/\hbar^2)\Delta r_{1\bar{1}0}$, where m^* is the electron effective mass. The rotation angle is thus proportional to the net displacement of electrons along the $[1\bar{1}0]$ axis, as recently discussed in Ref. 24. Hence, behind the spin relaxation process observed in the time-resolved analysis, there exists a spatially coherent pattern of spin polarization when each component is projected along the $[1\bar{1}0]$ net moving distance. Then, one can readily grasp the fact that an appropriate injection condition such as injection from a point contact or $(1\bar{1}0)$ plane can lead to a spatially coherent oscillation pattern of spin in a fixed spatial coordinate. In fact, the existence of such a pattern, which is called the persistent spin helix pattern, has been recently predicted in Ref. 19 and supported in theoretical analysis in Ref. 24. Our calculation showed that the spatial pattern also develops even at $\alpha\neq\beta$, though decoherence of spin polarization takes place and, in this regard, one requires a further analysis based on the space-resolved observation.

In the space-resolved analysis for the steady state, a time-averaged value of the spin polarization vector at each spatial coordinate, $\langle\mathbf{S}\rangle_T$, is the main concern. Although such an analysis basically requires two-dimensional observation of the spatial profile, the spin relaxation process with injection from a certain plane can be characterized by one-dimensional

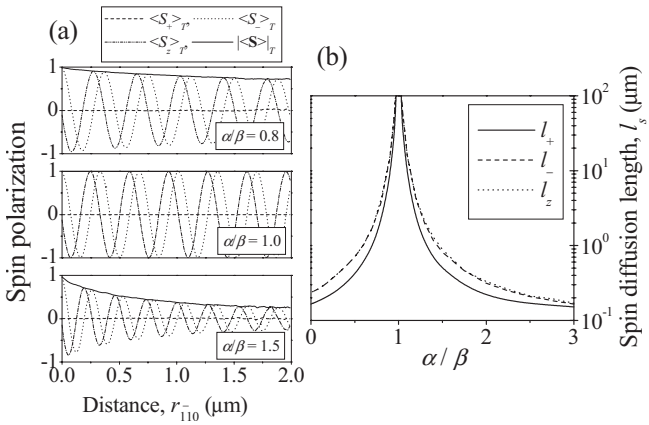

FIG. 3. (a) Spatial profiles of the time-averaged spin polarization vector at α/β=0.8 (top), 1.0 (middle), and 1.5 (bottom) with injected spin oriented in $[1\bar{1}0]$. (b) Dependence of the spin diffusion length l_s on α/β with different orientations of the injected spin polarization.

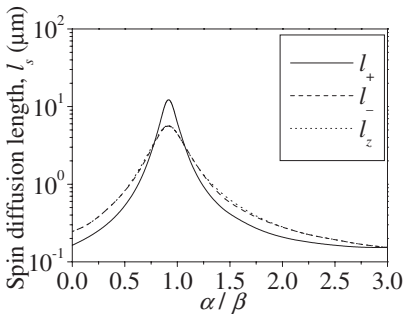

FIG. 4. Effect of the k^3 term on the spin diffusion length.

observation along the spatial coordinate perpendicular to the injection plane. This situation is closely related to the spin-FET structures,[5,6,20] and our focus here is placed on the process with injection from the $(1\bar{1}0)$ plane, in light of the fact that the spatial oscillation pattern develops along the $[1\bar{1}0]$ spatial coordinate as shown in Fig. 2(b). In all calculations, the width of the 2DEG system along the [110] spatial coordinate is assumed to be infinite.

Figure 3(a) represents the spatial profiles of $\langle \mathbf{S} \rangle_T$ during steady state when the electrons with spin oriented in $[1\bar{1}0]$ are injected from $r_{1\bar{1}0}$=0. In these calculations, the cubic term in the Dresselhaus model is neglected. The spatial oscillation of spin polarization is observed in all cases, and the spin relaxation takes place at α/β=0.8 and 1.5. Of utmost importance here is that no spin relaxation occurs at α/β =1.0 [middle graph in Fig. 3(a)] and that this spatial pattern is exactly equivalent to the PSH pattern.[19,24] This is the first confirmation of the existence of the PSH pattern based on the MC approach. When the injected spin is oriented in [001], the same behavior is observed except for the π phase shift in the spatial oscillation pattern. On the other hand, the injection of spin oriented in [110] yields a uniform spin distribution without any oscillation. The spatial profiles of $|\langle \mathbf{S} \rangle|_T$ in these cases can be approximated to be exponential decay characterized by "spin diffusion length." The dependence of the spin diffusion length l_s on the RD ratio is given in Fig. 3(b), where l_s with s=+, −, and z characterizes the steady state with injected spin oriented in [110], $[1\bar{1}0]$, and [001], respectively. The dotted line representing l_z is almost completely superimposed on the dashed line for l_-. One can see that all spin diffusion lengths become infinite at α/β=1.0, which is in marked contrast with the behavior of τ_s shown in Fig. 1. Moreover, within this range of the RD ratio, the spin diffusion lengths involving spatial oscillation, l_- and l_z, are always larger than the homogeneous case, l_+. In all cases, the spin relaxation at $\alpha \neq \beta$ is entirely ascribable to spin precession along $\Omega_{eff}(\mathbf{k})$ of which the orientation deviates from the [110] axis. The largest deviation is observed at $\mathbf{k} \| [110]$ where $\Omega_{eff}(\mathbf{k})$ is oriented in $[1\bar{1}0]$. The effective field $\Omega_{eff}(\mathbf{k}) \| [1\bar{1}0]$ always leads to decay of the homogeneous distribution of $\mathbf{S} \| [110]$, unless the spin experiences 2π rotation at $\mathbf{k} \| [110]$. On the other hand, when the spin is oriented in $[1\bar{1}0]$, the spin precession does not occur at $\mathbf{k} \| [110]$ and also there is no net moving distance of electron along the $[1\bar{1}0]$ spatial coordinate, which means no decay of the spatially coherent oscillation pattern. This could be one of the reasons why l_- and l_z are always larger than l_+ in Fig. 3(b). It should be pointed out that our calculations show that l_s obtained in the system with channel length of 4 μm is almost identical to the one with the channel length of 2 μm, which indicates that the size of the system does not influence the value of l_s.

The most important outcome in the present analysis is that the spin along any axis is totally suppressed at α/β=1.0. In this regard, it can be stated that the spin relaxation anisotropy vanishes at $\alpha=\beta$. This fact is expected to pave the way for realizing nonballistic spin-FETs with an operation scheme different from the one proposed in Ref. 5. For instance, by injecting spin oriented in the $[1\bar{1}0]$ axis, "on" and "off" states can be distinguished by the π phase shift in the spatially coherent pattern, which can be controlled by the small variation of the α value and, thus, by the small change of gate voltage, as is similar to the original proposal by Datta and Das.[6]

It is to be noted that total suppression of the spin relaxation is observed only when the spin orbit coupling consists of linear-in-**k** terms. As pointed out in Ref. 19, the most important contribution leading to the decay of the PSH is considered to be the cubic term of the Dresselhaus model. This term has been often neglected in the case of $k_F^2 \ll \langle k_z^2 \rangle$, and the effect of this term on the homogeneous spin distribution as well as the PSH pattern has not been well understood. The dependence of the spin diffusion length on the RD ratio calculated with the cubic term is shown in Fig. 4. It is seen that the divergent behavior of l_s vanishes in all cases. The peaks appear not at α/β=1 but at $\alpha/(\beta-\gamma k_F^2)$ =1.0 with $k_F^2=0.085\langle k_z^2 \rangle$. In the vicinity of the peak, the cubic term has a substantial impact on both the PSH pattern (l_- and l_z) and the spin homogeneous state (l_+). Yet the magnitude of spin diffusion lengths at $\alpha=\beta$ is considered to be

sufficiently large, compared to a typical device length of submicron order. Although a precise quantitative discussion requires more detailed simulation, for instance, including the Elliot-Yafet process,[3] the present result is quite suggestive of the possibility for a successful realization of Datt-Das-type spin-transistors[6] based on the (001) InAs QW system.

This work was partly supported by Grant-in-Aid for Scientific Research from the Japanese Ministry of Education, Culture, Sports, Science and Technology.

[1] M. I. D'yakonov and V. I. Perel', Sov. Phys. Solid State **13**, 3023 (1972).
[2] G. L. Bir, A. G. Aronov, and G. E. Pikus, Sov. Phys. JETP **42**, 705 (1976).
[3] R. J. Elliot, Phys. Rev. **96**, 266 (1954); Y. Yafet, in *Solid State Physics*, edited by F. Seitz and D. Turnbull (Academic, New York, 1963), Vol. 14.
[4] A. W. Oberhauser, Phys. Rev. **92**, 411 (1953).
[5] J. Schliemann, J. C. Egues, and D. Loss, Phys. Rev. Lett. **90**, 146801 (2003).
[6] S. Datta and B. Das, Appl. Phys. Lett. **56**, 665 (1990).
[7] G. Dresselhaus, Phys. Rev. **100**, 580 (1955).
[8] Y. A. Bychkov and E. I. Rashba, JETP Lett. **39**, 78 (1984).
[9] N. S. Averkiev and L. E. Golub, Phys. Rev. B **60**, 15582 (1999).
[10] N. S. Averkiev, L. E. Golub, and M. Willander, J. Phys.: Condens. Matter **14**, R271 (2002).
[11] J. Kainz, U. Rössler, and R. Winkler, Phys. Rev. B **68**, 075322 (2003).
[12] Y. V. Pershin, Physica E (Amsterdam) **23**, 226 (2004).
[13] J. Cheng and M. W. Wu, J. Appl. Phys. **99**, 083704 (2006).
[14] N. S. Averkiev, L. E. Golub, A. S. Gurevich, V. P. Evtikhiev, V. P. Kochereshko, A. V. Platonov, A. S. Shkolnik, and Yu. P. Efimov, Phys. Rev. B **74**, 033305 (2006).
[15] A. A. Kiselev and K. W. Kim, Phys. Rev. B **61**, 13115 (2000).
[16] S. Pramanik, S. Bandyopadhyay, and M. Cahay, Phys. Rev. B **68**, 075313 (2003).
[17] A. Bournel, P. Dollfus, E. Cassan, and P. Hesto, Appl. Phys. Lett. **77**, 2346 (2000).
[18] M. Shen, S. Saikin, M. C. Cheng, and V. Privman, Math. Comput. Simul. **65**, 351 (2004).
[19] B. A. Bernevig, J. Orenstein, and S. C. Zhang, Phys. Rev. Lett. **97**, 236601 (2006).
[20] K. Yoh, M. Ferhat, A. Riposan, and J. M. Millunchick, in *Physics of Semiconductors*, edited by J. Menéndez and C. G. Van de Walle, AIP Conf. Proc. No. 772 (AIP, Melville, NY, 2005).
[21] D. H. Park and K. F. Brennan, J. Appl. Phys. **65**, 1615 (1989).
[22] W. Knap *et al.*, Phys. Rev. B **53**, 3912 (1996).
[23] This process cannot actually be described as single-exponential decay and this relaxation consists of two processes; the fast process in the early period (up to about $t=0.35$ ps) is followed by the relatively slow process. Such two processes were also observed at any value of the RD ratio when the initial spin is parallel to $[1\bar{1}0]$ or [001]. The fast and slow processes are associated with the first π rotation and $n\pi$ rotation with $n>1$, respectively, in the spatially coherent oscillation pattern. The spin relaxation times τ_- and τ_z in Fig. 1 correspond to the fast process.
[24] M. H. Liu, K. W. Chen, S. H. Chen, and C. R. Chang, Phys. Rev. B **74**, 235322 (2006).